Numerical modelling of the Portevin-Le Chatelier effect

Matthieu Mazière* — Jacques Besson* — Samuel Forest*
Benoit Tanguy* — Hervé Chalons — François Vogel****

** Centre des Matériaux*
Mines Paris, Paristech
CNRS UMR 7633, BP 87, F-91003 Evry
maziere@mat.ensmp.fr

*** Turbomeca, F-64511 Bordes*

ABSTRACT. *The model proposed by MacCormick (1989) describing dynamic strain aging is used for a nickel based superalloy. The model is presented for small deformations, and an analytical homogeneous solution is calculated for simple tension. Parameters for the nickelbased superalloy at 500 °C are obtained from tensile tests at constant strain rates. A linear perturbation analysis is performed to evaluate the critical strain (*i.e. *when serrations begin). The convergence toward this critical value of two numerical integration schemes of material law is studied for the simulation of a plate in tension.*

RÉSUMÉ. *Le modèle de comportement proposé par MacCormick (1989) décrivant le vieillissement dynamique des métaux est utilisé pour modéliser un superalliage à base de Nickel. Le modèle est présenté en petites déformations, une solution analytique homogène en traction simple est déterminée, et un jeu de paramètres pour le superalliage à 500 °C est identifié à partir d'essais de traction à déplacement imposé. La déformation critique d'instabilité pour laquelle les oscillations débutent est déterminée à l'aide d'une analyse de perturbation linéaire. Elle est utilisée pour évaluer la convergence de deux schémas numériques d'intégration de la loi de comportement pour la simulation d'une plaque en traction.*

KEYWORDS: *Portevin-Le Chatelier effect (PLC), strain ageing, Nickel based superalloys, stability.*

MOTS-CLÉS : *effet Portevin-Le Chatelier (PLC), vieillissement dynamique, superalliages à base de Nickel, stabilité.*

DOI:10.3166/REMN.17.761-772

1. Introduction

The macroscopic load/displacement tensile curve of many materials exhibits serrations. This discontinuous yielding, associated with the repeated propagation of bands of localized plastic strain rate in tensile specimens, is due to dynamic strain ageing (DSA). DSA can be associated with a negative strain rate sensitivity (SRS) of the material in some range of strain rate and temperature, which can be evidenced by performing tensile tests at various strain rates. DSA is related at a microscopic scale to dynamic interactions between mobile dislocations and diffuse process of solute atoms. First observations of this phenomenon have been reported by (Le Chatelier, 1909) in iron and steel between 80°C and 250°C; and by (Le Chatelier *et al.*, 1923) in aluminium alloys at room temperature. Many experimental evidences of the so called Portevin-Le Chatelier (PLC) effect in such materials may be found in the references of (Neuhäuser, 1990), or in the first seven articles of *Scripta Metallurgica et Materialia*, Vol. 29-9, 1993.

Articles dealing with observations of PLC and DSA in nickel based superalloys are less common, perhaps because of the temperatures at which these effects appear. Serrated yielding has been observed by (Dybiec *et al.*, 1991) in Inconel 718: they investigated the influence of heat treatments on the critical plastic strain (*i.e.* when serrations begin). In (Bhanu Sankara Rao *et al.*, 1995), PLC effect is observed on Inconel 718 during strain controlled low cycle fatigue test. On the same material, (Fournier *et al.*, 2001) evidenced the link between PLC effect and shear fracture. The serrated flow appears around 500°C, in air and under secondary vacuum. Finally, (Girardin *et al.*, 2004) outlines the role of hydrogen during strain ageing in Nickel based alloys.

Material models attempting to describe the DSA and the PLC effects may be separated into two main groups. (i) Kubin-Estrin (KE) models proposed first by (Kubin *et al.*, 1985) and extended by (Zbib *et al.*, 1988) are based on the macroscopic description of deformation bands. The negative SRS is explicitly defined and serrations are obtain from strain rate jumps. (ii) MacCormick (MC) models proposed by (MacCormick, 1989) and improved by (Mesarovic, 1995) are based on a microscopic description of the DSA based on an internal variable t_a called ageing time. The negative SRS and serrations are implicit consequences of constitutive equations. Some more sophisticated models, improving previous ones (Fressengeas *et al.*, 2005), can also be found among the numerous references given in (Rizzi *et al.*, 2004).

Both models have been used to perform finite element simulations of the PLC effect in different structures. KE type models have been used by (Tsukahara *et al.*, 1999) in 2D plates, by (Kok *et al.*, 2003) in 3D flat strips, and by (Benallal *et al.*, 2006) in 2D axisymmetrical smooth and notched tensile test specimens. MC type models have been used by (Zhang *et al.*, 2001) in 3D thin flat strips and round bars, by (Graff *et al.*, 2004) on 2D U-notched specimens, and by (Graff *et al.*, 2005) on V-notched and CT specimens.

Some of these studies give details on parameters used to perform simulations. But there is generally a lack of information concerning computation parameters : number of time steps in the non-linear computation, numerical schemes used... The present article focuses on the computation parameters needed to capture the critical strain in the simulation of a plate in tension. For that purpose, the MC model is presented, and an homogeneous solution is calculated. Parameters of Udimet 720 at 500°C are identified from stress versus strain rate plots. Simulations of plates in tension are performed with Zset F.E. program (Besson *et al.*, 1997) for a constant applied global strain rate equal to $10^{-3}s^{-1}$. A stability analysis of the model is performed : (i) from the 1D linear perturbation method, the theoretical critical plastic strain is obtained; (ii) from (Drucker, 1950; Hill, 1958) stability conditions, local and global loss of stability are detected in the numerical solutions. The experimental, theoretical, and numerical critical plastic strains are compared to validate model parameters. Finally, two different methods to integrate the constitutive equations are compared.

2. Material model

2.1. *Constitutive equations*

Constitutive equations of the material model are formulated in the small strain framework. The strain rate tensor $\dot{\underset{\sim}{\varepsilon}}$ is split into elastic and plastic contributions, the evolution of the latter being given by the yield function f.

$$\dot{\underset{\sim}{\varepsilon}} = \dot{\underset{\sim}{\varepsilon}}_e + \dot{\underset{\sim}{\varepsilon}}_p \quad [1]$$

$$f(\underset{\sim}{\boldsymbol{\sigma}}, p, t_a) = J_2(\underset{\sim}{\boldsymbol{\sigma}}) - R(p) - P_1 C_s(p, t_a) \quad [2]$$

$$R(p) = R_0 + Q\left(1 - e^{-bp}\right) \quad [3]$$

where $J_2(\underset{\sim}{\boldsymbol{\sigma}})$ is the second invariant of the stress tensor, $R(p)$ is the nonlinear hardening law, and $P_1 C_s(p, t_a)$ is the extra-hardening induced by strain ageing. The over-concentration of solute atoms around dislocations C_s is estimated as a function of both internal variables of the model : the cumulated plastic strain p and the ageing time t_a.

$$C_s(p, t_a) = C_m\left(1 - e^{-P_2 p^{\alpha} t_a^n}\right) \quad [4]$$

The maximal over-concentration is C_m. P_2 characterises the rate of saturation of solute atoms around dislocations. The intensity in stress of the ageing effect is characterized by parameter P_1 (unit MPa). In fact, only the product $P_1 C_m$ can be identified based on mechanical tests. The cumulated plastic strain rate $\dot{p}$ is computed from the following viscoplastic hyperbolic flow rule.

$$\dot{p} = g(f) = \dot{p}_0 \sinh\left(\frac{\langle f\rangle}{K}\right), \quad \langle f\rangle = \frac{\mathrm{abs(f)} + \mathrm{f}}{2} \quad [5]$$

where g is an invertible monotonic function. The ageing time increment is computed from an implicit evolution law in which appears the cumulated plastic strain rate $\dot{p}$.

$$\dot{t}_a = 1 - \frac{t_a}{w}\dot{p} \qquad [6]$$

where w is the increment of the plastic strain which is produced when all the stopped dislocations overcome their obstacles.

2.2. *Homogeneous solutions*

For a simple tension test in a plate at a constant strain rate $\dot{\varepsilon}_0$, variables are uniform in the structure before the critical plastic strain p_c. In the plastic domain, the cumulated plastic strain rate $\dot{p}$ is nearly constant while plastic deformation increases. Then the Equation [6] can be integrated analytically and provides an explicit expression of t_a, as a function of $\dot{\varepsilon}_0$ and p.

$$t_a(p) = \frac{w}{\dot{\varepsilon}_0}\left(1 - e^{-\frac{p}{w}}\right) + \frac{R_0}{E\dot{\varepsilon}_0}e^{-\frac{p}{w}} \qquad [7]$$

The uniaxial tensile stress σ^{1D} is then given as a function of the cumulated plastic strain p and rate $\dot{p}$ from Equations [2], [4], [5].

$$\begin{aligned}\sigma^{1D}(p) = K\text{arcsinh}\left(\frac{\dot{p}}{\dot{p}_0}\right) + R_0 + Q\left(1 - e^{-bp}\right) \\ + P_1 C_m\left(1 - e^{-P_2 p^{\alpha} t_a(p)^n}\right)\end{aligned} \qquad [8]$$

This expression is useful for the stability analysis performed in the next section. Indeed, σ^{1D} coincides with the response of the tensile plate before the critical plastic strain. Some particular states of the material can be underlined, corresponding to specific values of t_a and σ^{1D}. The min. and max. solutions correspond respectively to virgin and fully aged states of the material. They represent the upper and lower limits for serrations, while the extra-hardening is either null either equal to $P_1 C_m$. Another solution corresponds to elastic loading/unloading, when ageing time increment $dt_a = dt$. The final state is obtained for the constant value of $t_a = \frac{w}{\dot{\varepsilon}}$ reached when $p \to +\infty$. This is the asymptotic value of the homogeneous solution [7].

2.3. *Material model parameters*

Parameters presented in the Table 2.3 have been obtained from various simple tensile tests performed on cylindrical smooth tensile specimens for different applied

strain rates. The stress/strain curves have been smoothed in order to : (i) evaluate the hardening parameters R_0, Q, and b for the slowest test (ii) outline the negative strain rate sensitivity of the material by plotting stress/strain rate curves at different deformation values. Hardening, viscous (K, $\dot{p}_0$) and ageing (P_1C_m, P_2, α) parameters have been identified, from the experimental data on the stress/strain rate curve (see Figure 1). n and w are taken from (Graff *et al.*, 2005). The experimental curve at a constant strain rate of $10^{-3}\mathrm{s}^{-1}$ is plotted in Figure 2, with the min., max., and homogeneous solutions for the parameters given by the identification. The experimental solution is accurately limited by the max. and min. solutions, and differs from the homogeneous one as soon as serrations begin. One can observe that $p_c^{EXP} \approx 0.8\%$.

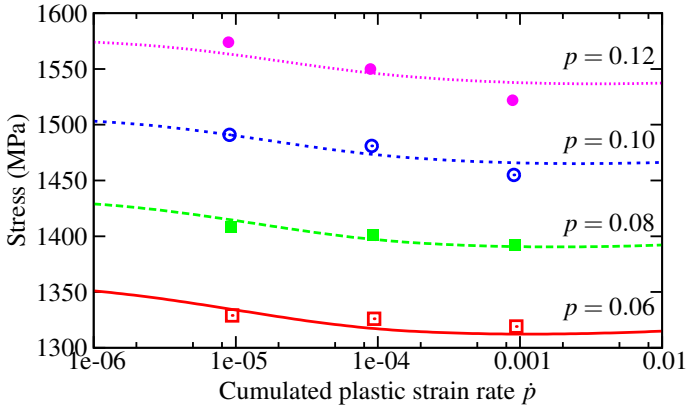

Figure 1. *Stress as a function of strain rate for experimental points and analytical curves for parameters given in Table 2.3. The model fits the experimental negative strain rate sensitivity in the range* $[10^{-5}\mathrm{s}^{-1}, 10^{-3}\mathrm{s}^{-1}]$ *for different plastic strain values*

Table 1. *Material model parameters identified for the nickel based superalloy at 500°C*

Elasticity	Hardening	Viscosity	Ageing
E 200 GPa	R_0 1046 MPa	K 1.55 MPa	P_1C_m 96 MPa
ν 0.3	Q 2200 MPa	$\dot{p}_0$ 10^{-4} s^{-1}	P_2 4.1 s^{-n}
	b 1.88		α 0.55
			n 0.33
			w 10^{-4}

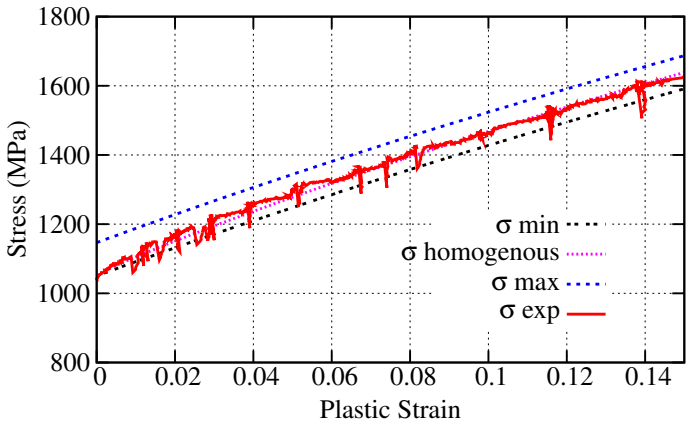

Figure 2. *Homogeneous, minimum, and maximum solutions, compared with an experimental simple tension test for the nickel based super-alloy at 500°C. The strain rate is for each solution equal to* $10^{-3}s^{-1}$

2.4. *Tension of a plate*

The specimen geometry is a $12.5mm \times 2.5mm$ plate, meshed with 2D 8 nodes plane stress elements with reduced integration (4 Gauss points). The numerical solution of this problem for a constant applied global strain rate equal to 10^{-3}s^{-1} is drawn in Figure 3. The critical plastic strain p_c, obtained from the stability analysis performed further, is indicated on the stress/strain curve. The maps of cumulated plastic strain rate $\dot{p}$ and of ageing time t_a are drawn on the structure for a global applied strain $\varepsilon = 3.2\%$. The analytical homogeneous solution coincides with the numerical solution before instability occurs, and the numerical critical plastic strain is close to the experimental value : $p_c^{NUM} \approx 0.82\%$. This critical plastic strain is evaluated from the criterion [12], which detects the loss of homogeneity of the solution in the plate. The good agreement between experimental and numerical values of the critical plastic strain is obtained adjusting the material model parameter α. The 1D linear perturbation analysis presented section 3.1 is performed for different values of α, in order to determine which value returns a theoretical critical plastic strain in agreement with experimental results.

3. Stability analysis

In this section, the 1D linear perturbation analysis provides a method to predict the theoretical critical cumulated plastic strain p_c. Stability conditions help to detect the corresponding numerical value in the 2D simulation. The critical plastic strain provided by finite element simulations is highly related to the method and the time

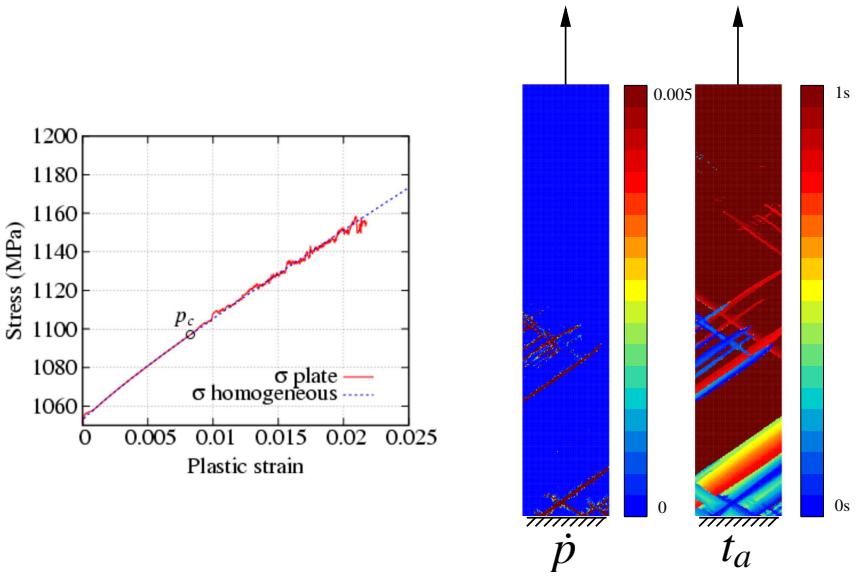

Figure 3. *Homogeneous analytic solution and numerical solution of a tensile plate at 500°C. The strain rate is constant and equal to* $10^{-3}\mathrm{s}^{-1}$. *The plastic strain is* 0.022

increments in the integration of constitutive equations. The numerical value of the critical plastic strain have to coincide with the theoretical approach to validate simulations.

3.1. *1D linear perturbation*

The 1D linear perturbation method consists in applying a perturbation $(\delta p, \delta t_a)$ to a homogeneous solution in a infinite medium of a given material (MacCormick, 1989; Mesarovic, 1995). For a given material and a given state of the structure - here a simple tension at a given strain rate - this method predicts the critical plastic strain p_c for which instabilities may occur. The stability of the medium is evaluated from the evolution of the perturbation rate $(\delta\dot{p}, \delta\dot{t}_a)$.

$$\begin{pmatrix} \delta\dot{p} \\ \delta\dot{t}_a \end{pmatrix} = [\mathbf{M}].\begin{pmatrix} \delta p \\ \delta t_a \end{pmatrix} = G(\dot{p})\begin{pmatrix} A(p,t_a) & B(p,t_a) \\ C(p,t_a) & D(p,\dot{p},t_a) \end{pmatrix}.\begin{pmatrix} \delta p \\ \delta t_a \end{pmatrix} \qquad [9]$$

Terms of the transition matrix $[\mathbf{M}]$ are calculated from the analytical homogeneous solution [7 - 8].

$$\left\{ \begin{array}{l} G(\dot{p}) = -g' = -\dfrac{dg}{df};\ A(p,t_a) = \dfrac{\partial(R+P_1C_s)}{\partial p};\ B(p,t_a) = \dfrac{\partial(P_1C_s)}{\partial t_a} \\ C(p,t_a) = -\dfrac{t_a}{w}\dfrac{\partial(R+P_1C_s)}{\partial p};\ D(p,\dot{p},t_a) = -\dfrac{t_a}{w}\dfrac{\partial(P_1C_s)}{\partial t_a} + \dfrac{\dot{p}}{w}\dfrac{1}{g'} \end{array} \right. \quad [10]$$

Eigenvalues of the matrix $[\mathbf{M}]$ linking $(\delta p, \delta t_a)$ to $(\delta\dot{p}, \delta\dot{t}_a)$ are evaluated. The stability is lost when these eigenvalues become purely real and positive (MacCormick, 1989). Eigenvalues λ of $[\mathbf{M}]$ are solutions of :

$$\begin{array}{l} \lambda^2 + 2\Phi\lambda + \lambda_0^2 = 0 \text{ with,} \\ \Phi = -G\left[\dfrac{A+D}{2}\right];\ \lambda_0^2 = G^2\left[AD - BC\right] > 0;\ \Delta = \Phi^2 - \lambda_0^2 \end{array} \quad [11]$$

The existence of real eigenvalues depends on the sign of Δ. If $\Delta > 0$, eigenvalues are real. If $\Delta < 0$, eigenvalues are complex and the sign of their real parts is the sign of $-\Phi$. For a given constant strain rate, three types of eigenvalues exist. This type depends on the plastic strain rate value, as represented in Figure 4. In area ⓐ, eigenvalues are complex with a negative real part, the perturbation evolves in a sinusoidal decreasing manner. In area ⓑ, eigenvalues are complex with a positive real part, the perturbation evolves in a sinusoidal increasing manner. In area ⓒ, eigenvalues are real and positive, the perturbation evolves in an exponential increasing manner. (MacCormick, 1989) has shown that the instability occurs when eigenvalues become real. Then, for a constant strain rate equal to 10^{-3}s^{-1}, the theoretical critical plastic strain rate is $p_c^{TH} = 0.8\%$ (cf. Figure 4), that is close to the experimental value.

3.2. *Stability conditions*

During the stable homogeneous evolution, ageing time t_a tends slowly towards its asymptotic value $\dfrac{w}{\dot{\varepsilon}}$. When serrations begin, most of the structure is submitted to elastic unloading ($dt_a = dt$), while plastic strain rate is concentrated in bands where t_a falls down to 0. An accurate tool to detect such unstable areas is the condition of negative second order work (Drucker, 1950; Hill, 1958) :

$$\dot{\underset{\sim}{\boldsymbol{\sigma}}} : \dot{\underset{\sim}{\boldsymbol{\varepsilon}}} < 0 \quad [12]$$

Even if this condition is fulfilled locally, the global stability of the structure is ensured as long as global stability condition is satisfied (Hill, 1958):

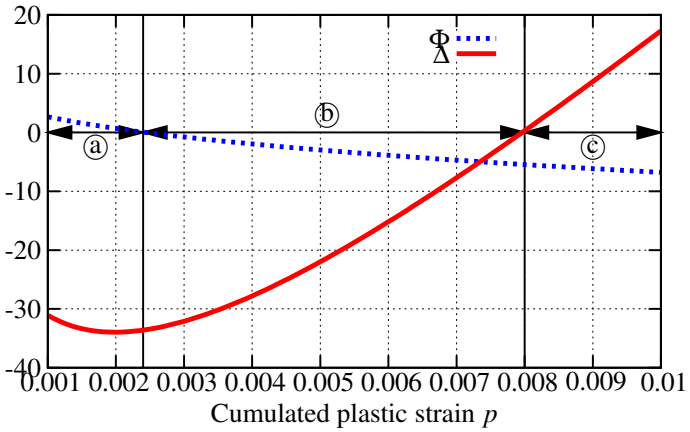

Figure 4. *Bifurcation diagram for a simple tensile state at a constant strain rate equal to* $10^{-3}s^{-1}$

Equilibrium is stable if $\forall \underline{\boldsymbol{V}}$ *kinematically admissible to 0,*

$$\int_{\Omega} \left(\dot{\underset{\sim}{\boldsymbol{\sigma}}} : \dot{\underset{\sim}{\boldsymbol{\varepsilon}}}(\underline{\boldsymbol{V}}) \right) dv > 0 \qquad [13]$$

Local instabilities coincide with drops of t_a (cf. Figure 5(a)). Global instabilities are accompanied with serrations on the global load/displacement curve, i.e. when the external load decreases. The frequency and intensity of drops of the external load can be measured from the global stability condition (cf. Figure 5(b)). In most cases, the "local instability" (first drop of t_a) occurs just before the global one (begin of serrations). The local instability condition provides a good estimate of the critical strain. Indeed, for a global strain rate of $10^{-3}s^{-1}$, the numerical plastic strain is $p_c^{NUM} \approx 0.82\%$, that is close to experimental and theoretical values.

4. Comparison of time integration methods

In this section, two numerical methods for the integration of constitutive equations are presented and compared, in terms of global time increment sensitivity of the results. The first integration method is an explicit fourth order Runge Kutta method with automatic time stepping. The second one is an implicit mid-point method (Θ-method) solved by a Newton-Raphson method, improved by the local switch to the Runge Kutta method. Simulations have been performed with the same precision for both methods, at a constant strain rate $\dot{\varepsilon} = 10^{-3}\mathrm{s}^{-1}$, for different values of the maximum

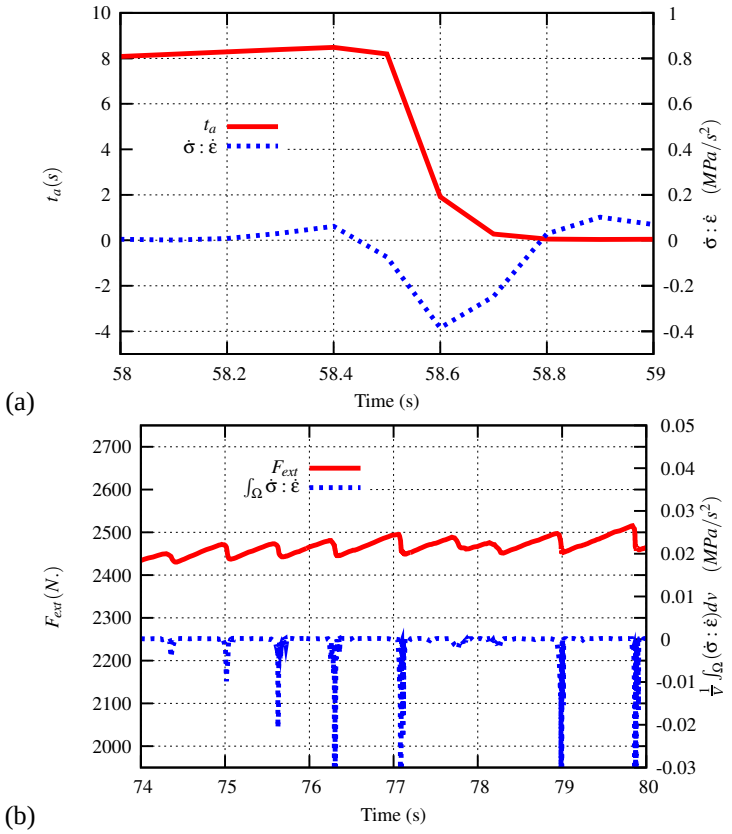

Figure 5. *(a) Local indicator (second order work) and ageing time at a given Gauss Point (b) Global indicator and load applied on the structure for a tensile plate simulation at a global strain rate equal to* $10^{-3}s^{-1}$

allowed global strain increment $\Delta\varepsilon_{max}$ per global increment. For each method the value of the critical cumulated plastic strain p_c, for which the numerical local instability occurs is evaluated. One can observe in Figure 6 that (i) the Θ-method is more efficient than the Runge Kutta one for a given $\Delta\varepsilon_{max}$ (ii) a small value of $\Delta\varepsilon_{max}$ is needed to capture an accurate value of the critical plastic strain.

5. Conclusion

An original method to evaluate parameters of the MC model is presented. Parameters have been validated from a stability analysis based on the linear perturbation method, and from finite element simulations of a plate in tension. Two methods of

time integration of constitutive equations are compared for their ability to accurately predict the critical plastic strain. Using the Θ-Method, an accurate value of the critical plastic strain is obtained for a maximal strain increment below 10^{-4}. This value can arbitrary be taken as a reference value for the maximum increment of global strain increment for simulations performed using parameters given in this article.

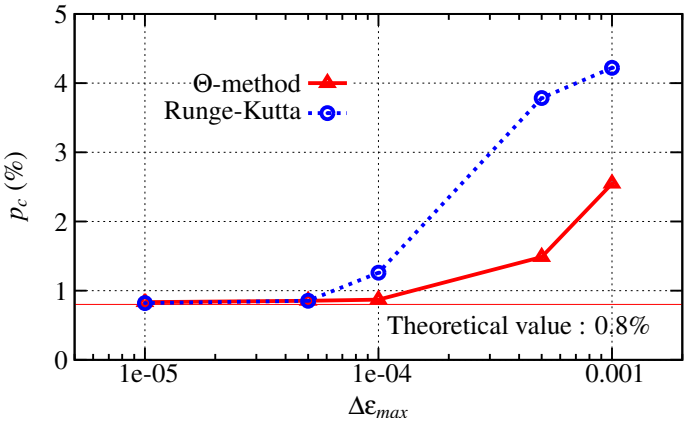

Figure 6. *Critical plastic strain p_c provided by Runge-Kutta method and modified Θ-Method for the simulation of a plate in tension at a given strain rate equal to $10^{-3}s^{-1}$. Simulations are performed for different values of $\Delta\varepsilon_{max}$*

6. References

Benallal A., Berstad T., Clausen A., Hopperstad O., " Dynamic strain aging and related instabilities : experimental, theoretical and numerical aspects", *Eur. J. Mech.*, vol. 25, p. 397-424, 2006.

Besson J., Foerch R., " Large scale object–oriented finite element code design", *Comp. Meth. Appl. Mech. Engng*, vol. 142, p. 165-187, 1997.

Bhanu Sankara Rao K., Kalluri S., Halford G., McGaw M. A., " Serrated flow and deformation substructure at room temperature in Inconel 718 superalloy during strain controlled fatigue", *Scripta Metallurgica et Materialia*, vol. 32, p. 493-498, 1995.

Drucker D., " Some implications of work hardening and ideal plasticity", *Quaterly of Applied Mathematics*, vol. 7, p. 411-418, 1950.

Dybiec H., Chaturvedi M., " Serrated yielding in Inconel 718", *Archives of metallurgy*, vol. 36, p. 341-352, 1991.

Fournier L., Delafosse D., Magnin T., " Oxidation induced intergranular cracking and Portevin - Le Chatelier effect in nickel base superalloy 718", *Mat. Sci. and Eng.*, vol. 316, p. 166-173, 2001.

Fressengeas C., Beaudoin A., Lebyodkin M., Kubin L., Estrin Y., " Dynamic strain aging : A coupled dislocation-Solute dynamic model", *Mat. Sci. and Eng.*, vol. 51, p. 226-230, 2005.

Girardin G., Delafosse D., " Measurement of the satured dislocation pinning force in hydrogenated nickel and nickel base alloys", *Scripta Materialia*, vol. 51, p. 1177-1181, 2004.

Graff S., Forest S., Strudel J.-L., Prioul C., Pilvin P., Béchade J.-L., " Strain localization phenomena associated with static and dynamic strain ageing in notched specimen:experiments and finite element simulations", *Mat. Sci. and Eng.*, vol. 387, p. 181-185, 2004.

Graff S., Forest S., Strudel J.-L., Prioul C., Pilvin P., Béchade J.-L., " Finite element simulations of dynamic strain ageing effects at V-notches and crack tips", *Scripta Materialia*, vol. 52, p. 1181-1186, 2005.

Hill R., " A general theory of uniqueness and stability in elastic-plastic solids", *J. Mech. Phys. Solids*, vol. 6, p. 236-249, 1958.

Kok S., Bharathi M., Beaudoin A., Fressengeas C., Ananthakrishna G., Kubin L., Lebyodkin M., " Spatial coupling in jerky flow using polycrystal plasticity", *Acta materialia*, vol. 51, p. 3651-3662, 2003.

Kubin L., Estrin Y., " The Portevin Le Chatelier effect in deformation with constant stress rate", *Acta Metall.*, vol. 33, p. 397-407, 1985.

Le Chatelier A., " Influence du temps et de la température sur les essais au choc", *Revue de métallurgie*, vol. 6, p. 914-917, 1909.

Le Chatelier F., Portevin A., " Sur le phénomène observé lors de l'essai de traction d'alliages en cours de transformation", *C. R. Acad. Sci. Paris*, vol. 176, p. 507-510, 1923.

MacCormick P., " Theory of flow localisation due to dynamic strain ageing", *Acta Metall.*, vol. 36, p. 3061-3067, 1989.

Mesarovic S., " Dynamic strain aging and plastic instabilities", *J. Mech. Phys. Solids*, vol. 43, n° 5, p. 671-700, 1995.

Neuhäuser H., *Patterns, Defects and Material Instabilities*, Kluwer Academic Publishers, chapter Plastic instabilities and the deformation of metals, p. 241-276, 1990.

Rizzi E., Hähner P., " On the Portevin-Le Chatelier effect : theoretical and numerical results", *Int. J. Plasticity*, vol. 20, p. 121-165, 2004.

Tsukahara H., Iung T., " Piobert-Lüders and Portevin - Le Chatelier instabilities. Finite element modelling with ABAQUS", *J. Phys. IV*, vol. 9, p. 157-164, 1999.

Zbib H., Aifantis E., " On the localization and postlocalization behavior of plastic deformation.III. On the structure and velocity of the Portevin - Le Chatelier bands", *Res Mechanica*, vol. 23, p. 293-305, 1988.

Zhang S., Mccormick P., Estrin Y., " The morphology of Portevin- Le Chatelier bands : finite element simulation for Al-Mg-Si", *Acta Mater.*, vol. 49, p. 1087-1094, 2001.